

Pressure response of Ce(Ag, Ni)Sb₂ compounds

R. T. KHAN^a, R. GALOS^a, E. BAUER^{a,*}, B. POPESCU^b, A. GALATANU^b^a*Institute of Solid State Physics, Vienna University of Technology, A-1040 Vienna, Austria*^b*National Institute of Materials Physics, 77125 Magurele, Romania*

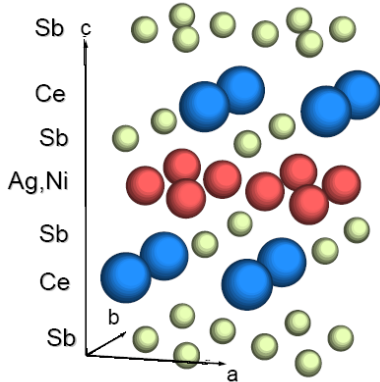
The pressure response of CeAg_{1-x}Ni_xSb₂ is studied by means of electrical resistivity measurements. The ferromagnetic ordering temperatures T_c of this series decrease as pressure is applied, except CeNiSb₂, showing a pressure driven continuous increase of T_c. This refers to crystalline electric field effects originating distinct different magnetic ground states. Concomitantly, the pressure response of various material dependent parameters also behave in the opposite direction.

(Received April 1, 2008; accepted June 30, 2008)

Keywords: Ce(Ag, Ni)Sb₂, pressure, Transport properties

1. Introduction

In many Ce and Yb based compounds, a competition of the Kondo effect (T_K) and the RKKY interaction strength (T_{RKKY}) reveals a wealth of emergent features like unconventional superconductivity, Fermi and non-Fermi liquid behaviour, magnetic order with substantially reduced ordered moments or intermediate valence states. In some cases, crystalline electric field (CEF) effects dramatically modify these appearances. Tetragonal ternary CeAgSb₂ (compare the crystal structure in Fig. 1) is one of the rare examples of a Kondo lattice exhibiting a ferromagnetically ordered ground state with T_c ≈ 9.6 K [1]. The ordered moments ($\mu_{\text{sat}} = 0.33 \mu_B/\text{Ce}$) are aligned along the c-axis [2], excellently matching the magnetisation data taken on a single crystal [3]. The large c/a ≈ 2.45 gives rise to strong anisotropic physical properties. Isostructural CeNiSb₂ is also reported to be ferromagnetic with T_c = 6 K, but the moments seem to be aligned along the a axis with an ordered moment almost twice as large as in the case of CeAgSb₂ [4]. The aim of the present study is to trace in some detail the evolution of the ground states when proceeding from FM-I CeAgSb₂ to FM-II CeNiSb₂. In order to complete this task, we have studied CeAg_{1-x}Ni_xSb₂ with x = 0, 0.33, 0.66 and 1 by means of externally applied pressure.

Fig. 1. Crystal structure of CeAgSb₂

2. Experimental

CeAg_{1-x}Ni_xSb₂ compounds (x = 0, 0.33, 0.67 and 1) have been prepared by RF melting in Ar atmosphere (starting with about 15% additional Sb to compensate for the Sb loss) and investigated by XRD (room temperature).

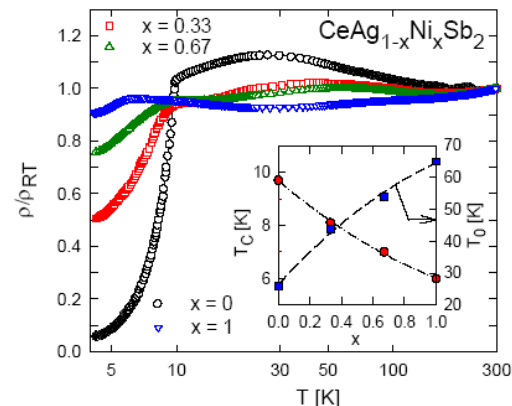


Fig. 2. Temperature dependent resistivity of CeAg_{1-x}Ni_xSb₂ for various concentrations x plotted in a normalised representation. The inset shows the concentration dependent evolution of T_c and of T₀.

All compounds were found to crystallize in the tetragonal ZrCuSi₂ type structure with the lattice parameter a slightly increasing from ≈ 4.37 Å to ≈ 4.39 Å, when Ag is substituted by Ni. Meanwhile the lattice constant c is decreasing from ≈ 10.70 Å to ≈ 9.75 Å, respectively. Electrical resistivity was measured in a 4-probe d.c. technique. Pressure was generated in a piston to cylinder cell made of MP35N, using Daphne oil as pressure transmitting media. Absolute pressure values were determined from the superconducting transition temperatures of lead.

3. Results and discussion

Fig. 2 summarises the temperature dependent electrical resistivity (ρ) of the samples investigated by plotting $\rho_{(T)}$ normalised to the respective room temperature values. The overall shapes of the $\rho_{(T)}$ curves are reminiscent of a Kondo lattice, modified by both CEF splitting and long range magnetic order. While the latter is responsible for a drop of $\rho_{(T)}$ in the low temperature range, coherence due to the lattice properties in the context of CEF splitting may be responsible for the local maxima (T_0) observed at elevated temperatures. Both characteristic temperatures are plotted as a function of concentration for CeAg_{1-x}Ni_xSb₂ in the inset of Fig. 2. Obviously, $T_c(x)$ smoothly decreases from 9.6 to 6 K when proceeding from $x = 0$ to $x = 1$. On the contrary, T_0 smoothly increases from about 30 K for $x = 0$ to more than 60 K for $x = 1$. In order to distinguish the ground state behaviour of both compounds, we have carried out pressure dependent resistivity measurements from about 1.5 K to room temperature and up to 20 kbar. Results are sketched in Figs. 3,4,5.

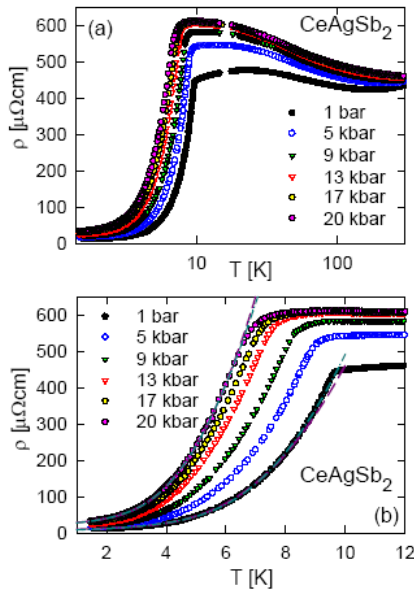


Fig. 3. Temperature and pressure dependent resistivity of CeAgSb₂ (upper panel). The lower panel shows low temperature details and least squares fits (dashed and dashed-dotted lines) for various concentrations x .

Fig. 3 shows a significant change of $\rho_{(T)}$ as magnetic order sets in. This allows unambiguously to determine $T_c(p)$ from a temperature derivative of the resistivity data. In agreement with a previously performed pressure study carried out on CeAgSb₂ [5], $\partial T_c/\partial p$ is negative for CeAgSb₂ with an initial slope $\partial T_c/\partial p|_i \approx -0.15$ K/kbar. This result coincides fairly well with $\partial T_c/\partial p$ derived from thermal expansion and specific heat measurements using the Ehrenfest relation [3]. Sidirov et al. [5] showed from their extended pressure range available that the quantum critical point, with $T_c = 0$, is reached for externally applied

pressure of about 50 kbar. Before T_c drops to zero, however, an antiferromagnetic phase is stabilized by growing pressure [5]. Similar trends of T_c and $\partial T_c/\partial p$ are observed for CeAg_{1-x}Ni_xSb₂ with $x = 0.33$ and $x = 0.67$. CeNiSb₂, however, behaves differently: the pressure response is positive, i.e., the magnetic ordering temperature increases as pressure increases, at least for pressures below 15 kbar. $\partial T_c/\partial p|_i \approx 0.1$ K/kbar. The remarkable different pressure response of the ordering temperatures obviously results from differences of the magnetic ground states of CeAgSb₂ and CeNiSb₂. The following observations may be key features: i) the more than two times larger magnetisation observed for CeAgSb₂ [6] (deduced at 6 T) is either the result of a distinct different CEF ground state doublet, and/or a dramatically different Kondo interaction strength. A reduced magnetic phase transition temperature as well as a

much larger paramagnetic Curie temperature for CeNiSb₂ [7], with $|\theta_p| \propto T_K$ would support the Kondo picture, too.

The substantially larger Kondo temperature for CeNiSb₂ also follows from a comparison of the magnetic entropy S_{mag} at $T = T_c$. While $S_{mag}(T = T_c) \approx R \ln 2$ for CeAgSb₂ [3], in the case of CeNiSb₂, $S_{mag}(T = T_c) \approx 0.5 R \ln 2$ [4]. The latter proves that entropy is spread out over a larger temperature range due to a larger Kondo temperature. The different orientation of the ordered moments refers to differences in the CEF scheme of both compounds. In fact, Takeuchi et al. and Thamizavel et al. [3,4] figured out that $|\pm 1/2\rangle$ is the ground state doublet for CeAgSb₂ while $|\alpha \pm 3/2\rangle + |\beta \pm 5/2\rangle$ is the ground state doublet of CeNiSb₂ ($\alpha = 0.531$, $\beta = 0.847$). The dramatic change of the crystal field ground state when proceeding from CeAgSb₂ to CeNiSb₂ cannot be explained in terms of simple point charge models; rather hybridisation may play a crucial role.

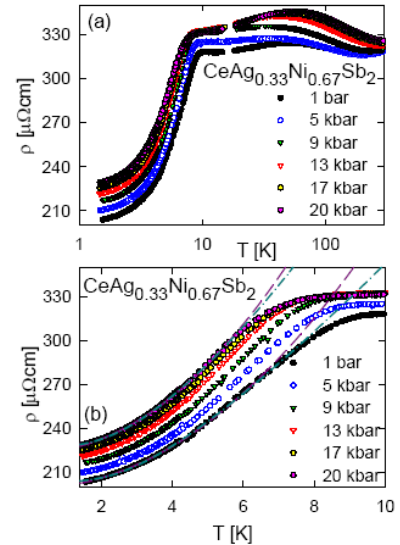


Fig. 4. Temperature and pressure dependent resistivity of CeAg_{0.33}Ni_{0.67}Sb₂ (upper panel). The lower panel shows low temperature details and least squares fits (dashed and dashed-dotted lines) for various concentrations x .

In order to analyse in more detail the magnetically ordered regime of the present series, we have used an expression discussed by Jobilong et al [8]. The respective model considers a ferromagnetic spin wave with a gap Δ in the magnon dispersion relation. This model yields:

$$\rho^{FM} = \rho_0 + AT^2 + BT\Delta \left(1 + \frac{2T}{\Delta} \exp(-\Delta/T)\right) \quad (1)$$

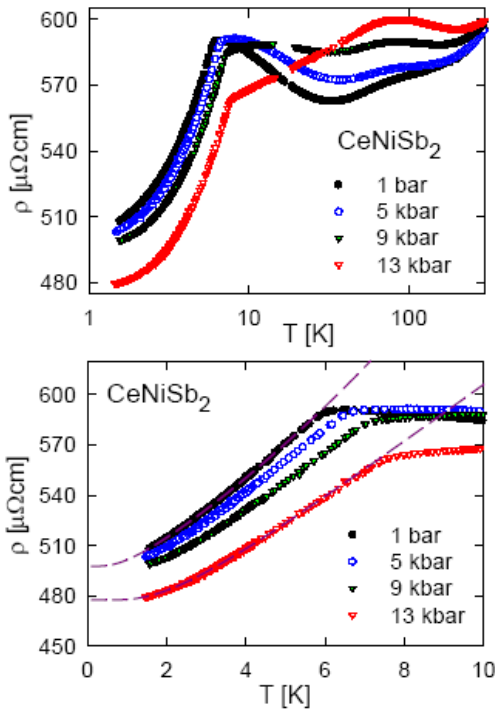


Fig. 5. Temperature and pressure dependent resistivity of CeNiSb_2 (upper panel). The lower panel shows low temperature details and least squares fits (dashed and dashed-dotted lines) for various concentrations x .

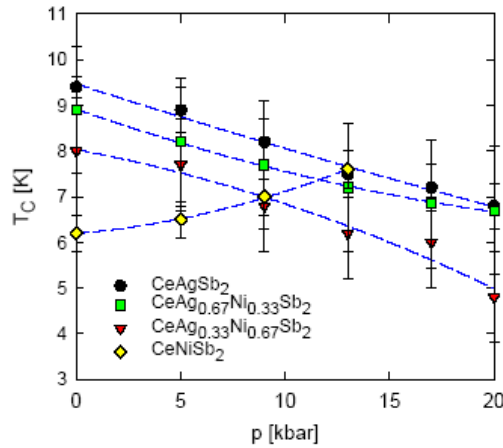


Fig. 6. Pressure dependent Curie temperatures T_c of $\text{CeAg}_{1-x}\text{Ni}_x\text{Sb}_2$. The lines are guides for the eyes.

If $\Delta \rightarrow 0$, $\rho - \rho_0 \sim T^2$. ρ_0 is the residual resistivity, AT^2 represents the Fermi liquid term, rendering scattering on heavy quasi-particles, and B is a material dependent constant. An analysis of the temperature and pressure dependent resistivity based on Eqn. 1 is rendered in Figs. 3, 4 and 5 (lower panels, dashed lines) and summarized in Fig. 7 for both A and Δ .

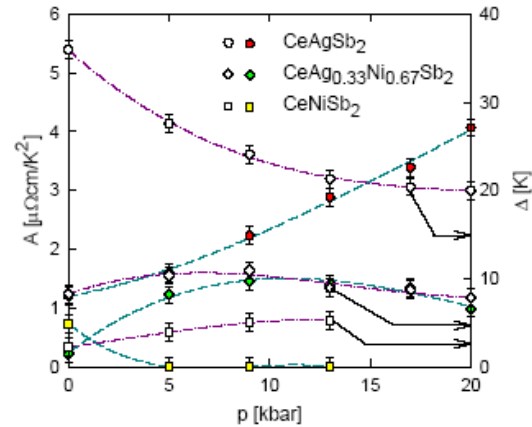


Fig. 7. Pressure dependence of the prefactor A and the gap width Δ of $\text{CeAg}_{1-x}\text{Ni}_x\text{Sb}_2$. The lines are guides for the eyes.

There is a number of interesting features observed: i) For Ag rich compounds, showing a decrease of the transition temperature as the pressure increase, the energy gap in the magnon dispersion relation, Δ , decreases as well. Particularly, the decrease of $\Delta(p)$ as derived from the present investigation fairly well agrees with previously performed studies [5]. For CeNiSb_2 , however, $\Delta(p)$ increases, emphasising once again the fundamental differences in the nature of the magnetically ordered ground state, although all these compounds are, macroscopically, ferromagnets. A very specific pressure response is found for the electron-electron interaction prefactor A . Since heavy quasi-particles are involved, $A \propto (N(E_F))^2$ is very large (of the order of $1 \mu\Omega\text{cm}/\text{K}^2$) at ambient conditions. In the case of CeAgSb_2 , $A(p)$ grows from $1 \mu\Omega\text{cm}/\text{K}^2$ ($p = 1$ bar) to more than $4 \mu\Omega\text{cm}/\text{K}^2$ for $p = 20$ kbar. In general, applying pressure to Ce systems causes an increase of the Kondo temperature T_K , consequently, $N(E_F) \propto 1/T_K$ is expected to decrease. This relation holds for simple Kondo systems if no further interaction mechanisms are considered. RKKY interaction and CEF effects, however, play a fundamental role in the compounds under consideration and can distinctly modify the above indicated simple relation. In the proximity of a magnetic instability, this relation may reverse and an increase of T_K may be attended by an increase of $N(E_F)$ as well. This follows from model calculations of the temperature dependent specific heat if long range magnetic order is described within the molecular field theory while the Kondo effect follows from the model of Schotte and Schotte [9–11]. The former is characterised by

a coupling constant J and the latter by T_K . These calculations reveal that for $T_K \geq 2J/\pi$

long range magnetic order vanishes, while $T_{\text{ord}} = J/2$ for $T_K = 0$ (only nearest neighbours are considered). For a recent discussion compare Ref. [12]. This model explains the $A(p)$ dependence observed experimentally for CeAgSb₂ in the magnetically ordered regime without restraint. The much larger Kondo temperature deduced for CeNiSb₂, however, may cause a dominance of the scattering on heavy quasiparticles, prior to that on excitations of the spin wave, which, tentatively, may originate the very strong decrease of $A(p)$ as the pressure raises. The substituted compound, CeAg_{0.33}Ni_{0.67}Sb₂, can be expected to behave intermediate. In fact, the present experimental data (compare Fig. 7) seem to corroborate this scenario. At low temperatures, $\rho(T)$ of the samples rich in Ag can also be accounted for by an antiferromagnetic model [8]:

$$\rho^{AFM} = \rho_0 + AT^2 + C\Delta^2 \exp(-\Delta/T) \left\{ \frac{1}{5} \left(\frac{T}{\Delta} \right)^5 + \left(\frac{T}{\Delta} \right)^4 + \frac{5}{3} \left(\frac{T}{\Delta} \right)^3 \right\}$$

where C is a constant and Δ is the gap in the antiferromagnetic spin wave dispersion. Least squares fits according to Eq. 2 are shown in Figs. 3 and 4 (lower panels) as dashed-dotted lines. The latter model reveals even better agreement with the data in a broader temperature range than fits using Eq. 1, at least for the samples rich in Ag. Eq. 2, however, totally fails to describe $\rho(T)$ for $T < T_c$ in the case of CeNiSb₂. This may refer to the fact that CeAgSb₂ and compounds rich in Ag are close to an antiferromagnetically ordered state, while CeNiSb₂ appears to be a good ferromagnet, at least from the present study. The former coincides with an AFM state of CeAgSb₂ observed at high pressure [5].

4. Summary

CeAg_{1-x}Ni_xSb₂ crystallises in the tetragonal ZrCuSiAs structure. Ferromagnetic order is found for CeAgSb₂ at $T_c = 9.6$ K as a consequence of a subtle balance of RKKY interaction, the Kondo effect and CEF splitting. As the Ni content increases, T_c reduces, reaching about 6 K in the case of CeNiSb₂. Increasing hybridisation of conduction electrons with the Ce-4f moments also brings about an alteration of the 4f wave function of the CEF ground state, changing from a $\pm|1/2\rangle$ state to a mixture of $\pm|3/2\rangle$ and $\pm|5/2\rangle$ states for CeNiSb₂. This also modifies the direction of the ordered moment, from a basal plane alignment in the case of CeAgSb₂ to a c-axis direction of the Ce moments in CeNiSb₂. Pressure applied to this series results in a nonmonotonous evolution of the magnetic ordering temperatures T_c , of the Fermi liquid prefactor A and of the

spin wave gap Δ , rendering changes of the CEF ground state.

Acknowledgements

This work was supported in part by the Austrian FWF P18054, by the Romanian CeEx projects RP5/2005, M3-204/2006 and M1-98/2006 and by the COST P-16 ECOM.

References

- [1] M. Houshiar, D. T. Adroja, B. D. Rainford, J. Magn. Magn. Mat. **140-144**, 1231 (1995).
- [2] Shingo Araki, Naoto Metoki, Andrei Galatanu, Etsuji Yamamoto, Arumugam Thamizhavel, Yoshichika Onuki, Phys. Rev. B **68**, 024408 (2003).
- [3] T. Takeuchi, Arumugam Thamizhavel, Tomoyuki Okubo, Mineko Yamada, Noriko Nakamura, Takeshi Yamamoto, Yoshihiko Inada, Kiyohiro Sugiyama, Andrei Galatanu, Etsuji Yamamoto, Koichi Kindo, Takao Ebihara, Yoshichika Onuki, Phys. Rev. B **67**, 064403 (2003).
- [4] Arumugam Thamizhavel, Tetsuya Takeuchi, Tomoyuki Okubo, Mineko Yamada, Rihito Asai, Shingo Kirita, Andrei Galatanu, Etsuji Yamamoto, Takao Ebihara, Yoshihiko Inada, Rikio Settai, Yoshichika Onuki, Phys. Rev. B **68**, 054427 (2003).
- [5] V. A. Sidorov, E. D. Bauer, N. A. Frederick, J. R. Jeffries, S. Nakatsuji, N. O. Moreno, J. D. Thompson, M. B. Maple, and Z. Fisk, Phys. Rev. B **67**, 224419 (2003).
- [6] B. Popescu, E. Royanian, H. Michor, G. Hilscher, E. Bauer and A. Galatanu, Physica B, **403**(5-9), 937 (2008).
- [7] Yuji Muro, Naoya Takeda and Masayasu Ishikawa, J. Alloys and Compounds **257**, 23 (1997).
- [8] E. Jobilong, J. S. Brooks, E. S. Choi, H. Lee and Z. Fisk, Phys. Rev B **72**, 104428 (2005).
- [9] K. D. Schotte and U. Schotte, Phys. Lett. **55 A**, 38 (1975).
- [10] A. Braghta PhD Thesis, University of Strasbourg (1989).
- [11] M. J. Besnus, A. Essaihi, G. Fischer, N. Hamdaoui, A. Meyer, J. Magn. Magn. Mat. **104 – 107**, 1385 (1992).
- [12] A Gribanov, A Tursina, E Murashova, Y Seropegin, E Bauer, HKaldarar, R Lackner, H Michor, E Royanian, M Reissner and P Rogl, J. Phys.: Condens. Matter **18**, 9593 (2006).

*Corresponding author. bauer@ifp.tuwien.ac.at